

SCIENTIFIC REPORTS



OPEN

Metabolomic and lipidomic plasma profile changes in human participants ascending to Everest Base Camp

Katie A. O'Brien^{1,2}, R. Andrew Atkinson³, Larissa Richardson⁴, Albert Koulman⁴, Andrew J. Murray², Stephen D. R. Harridge¹, Daniel S. Martin^{5,6}, Denny Z. H. Levett^{7,8}, Kay Mitchell^{7,8}, Monty G. Mythen⁹, Hugh E. Montgomery^{5,10}, Michael P. W. Grocott^{7,8}, Julian L. Griffin¹¹ & Lindsay M. Edwards^{1,12}

At high altitude oxygen delivery to the tissues is impaired leading to oxygen insufficiency (hypoxia). Acclimatisation requires adjustment to tissue metabolism, the details of which remain incompletely understood. Here, metabolic responses to progressive environmental hypoxia were assessed through metabolomic and lipidomic profiling of human plasma taken from 198 human participants before and during an ascent to Everest Base Camp (5,300 m). Aqueous and lipid fractions of plasma were separated and analysed using proton (¹H)-nuclear magnetic resonance spectroscopy and direct infusion mass spectrometry, respectively. Bayesian robust hierarchical regression revealed decreasing isoleucine with ascent alongside increasing lactate and decreasing glucose, which may point towards increased glycolytic rate. Changes in the lipid profile with ascent included a decrease in triglycerides (48–50 carbons) associated with *de novo* lipogenesis, alongside increases in circulating levels of the most abundant free fatty acids (palmitic, linoleic and oleic acids). Together, this may be indicative of fat store mobilisation. This study provides the first broad metabolomic account of progressive exposure to environmental hypobaric hypoxia in healthy humans. Decreased isoleucine is of particular interest as a potential contributor to muscle catabolism observed with exposure to hypoxia at altitude. Substantial changes in lipid metabolism may represent important metabolic responses to sub-acute exposure to environmental hypoxia.

Reduced cellular oxygen availability (hypoxia) is a feature of many disease states. Oxygen delivery may be globally impaired by diseases of the heart or lung, or by anaemia (in which the concentration of oxygen-carrying haemoglobin is reduced); or regionally or locally impaired by macrovascular and microvascular disease respectively^{1,2}. Diffusion of oxygen in the lungs and/or tissues may be impaired through accumulation of parenchymal fluid and/

¹Centre for Human and Applied Physiological Sciences, King's College London, London, UK. ²Department of Physiology, Development and Neuroscience, University of Cambridge, Downing Street, Cambridge, UK. ³Centre for Biomolecular Spectroscopy and Randall Division of Cell and Molecular Biophysics King's College London Guy's Campus London, London, UK. ⁴NIHR BRC Nutritional Biomarker Laboratory, University of Cambridge, Pathology building level 4, Addenbrooke's Hospital, Cambridge, UK. ⁵University College London Centre for Altitude Space and Extreme Environment Medicine, UCLH NIHR Biomedical Research Centre, Institute of Sport and Exercise Health, First Floor, 170 Tottenham Court Road, London, W1T 7HA, UK. ⁶Critical Care Unit, Royal Free Hospital, Pond Street, London, NW3 2QG, UK. ⁷Southampton NIHR Biomedical Research Centre, University Hospital Southampton, Southampton, UK. ⁸Integrative Physiological and Critical Illness Group, Division of Clinical and Experimental Science, Faculty of Medicine, University of Southampton, Southampton, UK. ⁹University College London Hospitals National Institute of Health Research Biomedical Research Centre, London, UK. ¹⁰Centre for Human Health and Performance, Department of Medicine, University College London, London, UK. ¹¹Department of Biochemistry and Cambridge Systems Biology Centre, University of Cambridge, Tennis Court Road, Cambridge, UK. ¹²Respiratory Data Sciences Group, Respiratory TAU, GlaxoSmithKline Medicines Research, Stevenage, UK. Correspondence and requests for materials should be addressed to K.A.O. (email: ko337@cam.ac.uk) or L.M.E. (email: lindsay.m.edwards@gsk.com)

or inflammatory changes¹. Meanwhile, ascent to high altitude resulting in exposure to environmental hypobaric hypoxia may also reduce tissue oxygen availability: the associated fall in barometric pressure is in turn associated with a decrease in the inspired partial pressure of oxygen (PO₂). Increasing numbers of lowlanders travel to high altitude destinations, whilst ~7% of the world's population (440 million people) reside above 1500 m³).

Adjustment to hypoxic conditions (acclimatisation) involves responses that mitigate reduced oxygen delivery, including an increase in minute ventilation and erythropoiesis⁴. Acclimatisation also requires a metabolic response to help match ATP synthesis and demand in the face of decreased oxidative capacity and increased oxidative stress^{5–7}.

To date, studies examining metabolic acclimatisation in healthy human lowlanders have predominantly focused upon tissue specific responses, particularly those of skeletal muscle. These suggest a shift away from oxidative processes including β -oxidation, TCA cycle activity and oxidative phosphorylation (reviewed in⁵) and towards increased reliance upon carbohydrate metabolism. Enhanced glycolytic capacity has been suggested by increased intramuscular levels of glycolytic intermediates⁸ and hypoxic inducible factor 1- α (HIF-1 α) mediated upregulation of glucose transporters and glycolytic enzymes^{9,10}.

Hypoxia-induced alterations to lipid storage and mobilisation include a fall in circulating high density lipoproteins alongside increased triglyceride (TG) concentrations¹¹, inhibition of lipoprotein lipase activity¹² and suppression of *de novo* lipogenesis^{13,14}. These responses are likely to be mediated at the transcriptional level through HIF-1/2 α ^{15–17} and may be affected by changes in circulating catecholamines^{6,11}, which are known to stimulate lipolysis via hormone sensitive lipase¹⁸. In addition, a transcriptional regulator of fatty acid oxidation in the liver, heart and muscle, peroxisome proliferator activated receptor α (PPAR α), has been identified as a key regulator of hypoxic metabolic remodeling processes, with the metabolic adaptations of native high altitude Sherpa populations being linked to a putatively advantageous allele for the PPAR α gene^{8,19,20}.

Whilst details on metabolic acclimatisation to hypoxia are emerging, there are profound differences between studies in the duration and degree of hypoxic exposure⁵, which tends to be applied to highly selected, small groups of participants (e.g. ^{21,22}). Amongst those involving larger cohorts, there has been a failure to use standardised ascent profiles^{23–25}. Further, many studies have been tissue-specific, with little attention paid to circulating features indicative of global systemic metabolic responses.

Metabolomic and lipidomic analyses of biofluids measure a large number of variables of interest within the metabolic and lipid systems, thus providing a sensitive measure of functional biological phenotype (reviewed in²⁶). The power of such analyses has been demonstrated in the identification of biomarkers related to the diagnosis or prognosis of a range of diseases²⁷. The application of such methodology to the examination of responses to human hypobaric hypoxia has the potential to elucidate a metabolic signature of altitude exposure^{28,29}. The few studies that have adopted this approach in the context of high altitude exposure have again employed small, select study cohorts^{30,31}.

In order to better describe the human response to hypobaric hypoxia, we thus performed a large scale prospective metabolomic and lipidomic analysis of plasma samples taken from 198 participants across 5 timepoints upon their ascent to Everest Base Camp (EBC, 5,300 m) as part of the Caudwell Xtreme Everest expedition³².

Methods

The study design, risk management plan and individual protocols for the Caudwell Xtreme Everest (CXE) Expedition were approved by the University College London (UCL) Research Ethics Committee (in accordance with the declaration of Helsinki). All methods were performed in accordance to relevant guidelines and regulations. The study was designed and conducted by the UCL Centre for Altitude Space and Extreme Environment Medicine (CASE). Both verbal and written informed consent was obtained from all participants.

Participants. Details on subject recruitment and characteristics have been outlined previously³². Briefly, participants included males and females aged over 18 with no upper age limit, who were required to pass two separate health screening stages³². From this screening process, 198 healthy volunteers participated in the study.

Study design. Ascent profiles, details on logistics as well as barometric pressure (P_B), inspired partial pressure of oxygen (P_iO₂) and temperature at the respective altitude laboratories have been reported previously³². Baseline measurements were performed in London (LDN) in a laboratory at UCL (75 m above sea level, P_iO₂ 19.7 KPa) between January 4th and February 26th 2007. Field studies were performed between 31st March and 6th June 2007 at laboratories set up at the following locations (altitudes expressed as meters, m): Kathmandu (KTM, 1,300 m, P_iO₂ 16.8 KPa), Namche (NAM, 3,500 m, P_iO₂ 12.7 KPa), Pheriche (PHE, 4,250 m, P_iO₂ 11.6 KPa) and Everest Base Camp (EBC, 5,300 m, P_iO₂ 9.9 KPa). Data collection, including plasma sample collection, was performed at each of these time points.

All participants underwent an identical ascent profile, arriving at EBC on day 11. To maintain an identical pattern of hypoxic exposure, participants' movements were restricted on rest days, such that no subject ascended or descended more than 300 vertical meters from the laboratory altitude. The total trekking distance achieved over 11 days from Lukla airport to EBC was 50.7 km, with 5 days of rest over this course. The distance covered per day, taken at a gentle pace over the course of the day, was thus as follows: Lukla to NAM 9.1 km/day, NAM to PHE 10.3 km/day, PHE to EBC 5.9 km/day.

Physiological variables. Body weight and arterial O₂ saturation (SpO₂), were determined prior to any oral intake on the morning that blood samples were obtained⁶.

Plasma Sample Analysis. *Blood sampling.* All blood samples were taken on a rest day the morning after arrival at each altitude location, being a minimum of 16 hours post exercise. Subjects were in a rested, fasting state and blood was taken from the antecubital vein and collected in 10 ml BD ethylenediamine-tetra-acetic acid

(EDTA) blood tubes (Southern Syringe Services LTD). Plasma was separated from blood cells by centrifugation of whole blood at 800 g for 15 min and immediately frozen in 1 ml aliquots in liquid nitrogen. Samples were kept below -80°C until analysis.

Plasma preparation. Plasma samples were defrosted at room temperature. A 1:1:1 extraction was performed³³, with 500 μl of methanol (Hypergrade for LC-MS, Merck) and 500 μl of chloroform (HiPerSolv Chromanorm for HPLC, VWR international), both ice cold, being added to 500 μl of plasma in a 1.5 ml Eppendorf. This was vortexed for 2 min, left to stand at -20°C for 30 min, and then centrifuged for 3 min at 9100 g (Force 1624 Microcentrifuge) to yield upper (methanol/aqueous, fraction) and lower phases (chloroform/lipid, fraction). 700 μl of the upper phase and ~ 200 μl of the lower phase were pipetted into Eppendorf tubes for nuclear magnetic resonance spectroscopy (NMR) and mass spectrometry analysis, respectively.

Upper phase/methanol fraction. The upper fraction was dried down at 30°C for 4 hours using a vacuum centrifuge (Eppendorf Concentrator 5301) and then re-suspended in 600 μl of the following NMR buffer: double distilled H_2O containing 5% D_2O for NMR (Acros organics, CAS: 7789-20-0) and 1 mM 3-trimethylsilyl-1-propanesulfonic acid sodium salt (DSS) (Aldrich, 178837-5 G). D_2O was required for the magnetic lock frequency and DSS was used as a chemical shift reference. The resulting solution was transferred to 5 mm NMR tubes within a 96-tube rack.

Proton (^1H -) NMR spectral acquisition and processing. ^1H -NMR spectra of plasma samples were obtained using a Bruker Avance III 700 MHz spectrometer (Bruker Biospin, Karlsruhe, Germany) as described previously³⁴. All samples were analysed on a participant by participant basis, meaning that plasma taken from the same participant at all 5 time points was defrosted and treated at the same time and run within the same NMR experiment. This was to ensure any daily differences in experimental procedure were removed from analysis when data between time points were compared.

Resulting spectra were processed using TopSpin (Bruker, Karlsruhe, Germany). Spectra were converted from time to frequency domain using a Fourier transform. The phase was adjusted and spectra aligned so that the DSS peak corresponded to 0 ppm through use of the *icoshift* program in Matlab³⁵. Due to the degree of noise present, the aromatic region was excluded and only the aliphatic spectral region analysed. Normalisation and scaling of this spectral region were performed through use of Probabilistic Quotient normalisation³⁶ and Pareto scaling³⁷, respectively (Supplementary Fig. 1).

Initial principal components analysis (PCA) on this region revealed a separation into two regions that was not due to variation dependent on the experiment i.e. a change with location and thus with altitude (Supplementary Fig. 2). Instead, it was likely due to sample acquisition differences such as slight alterations in gain between NMR batch runs, as the samples were run in two batches at different times. A bias trend was identified to capture 77% of this variance (Supplementary Fig. 3) and was subsequently normalised using EigenMS (Supplementary Fig. 4)^{38–40}. As all samples from any single subject were run at the same time, they were contained within one of the two batch effect groups.

Following this, the full resolution spectra were binned at a ratio of 10:1. This ratio was found to sufficiently reduce the size of the data set, whilst retaining maximal information. The total number of bins was 1203. Putative identification of the metabolites associated with the peaks undergoing significant changes was undertaken using Chemomx software (Chemomx NMR Suite 7.1).

Lower phase/lipid fraction analysis by direct infusion mass spectrometry (DIMS). All solvents used were of LC-MS grade or better and were ordered from Sigma Aldrich (Gillingham, UK). Quality controls (QC's) were derived from pooling all samples and serially diluting with chloroform. Internal standards for key lipid species or blanks (either PBS or chloroform) were prepared to run alongside the sample lipid fraction. All internal standards were obtained from Avanti Polar Lipids (Alabaster, AL, USA) with the exception of undecanoic acid and trilaurin (Sigma Aldrich).

The sample, QC's and blanks (30 μl) were placed in a pre-defined random order across 96-well plates (Plate+, Esslab, Hadleigh, UK). To this, 750 μl methyl tert-butyl ether (MTBE) was added, along with 150 μl of internal standard mix, containing the following six internal standards: 1,2-di-o-octadecyl-sn-glycero-3-phosphocholine (0.6 μM), 1,2-di-O-phytanyl-sn-glycero-3-phosphoethanolamine (1.2 μM), C8-ceramide (0.6 μM), N-heptadecanoyl-D-erythro-sphingosylphosphorylcholine (0.6 μM), undecanoic acid (0.6 μM), and trilaurin (0.6 μM). The blanks remained as such through addition of 150 μl chloroform instead of internal standard. The plate was subsequently shaken for 30 s.

Using a VIAFLO 96/384 electronic pipette (Integra), 25 μl of the resulting sample mixture was transferred to a glass coated 384 well plate and 90 μl mass spectrometry (MS) mix [7.5 mM NH_4Ac IPA:MeOH (2:1)] added. The plates were then sealed using Corning aluminium micro-plate sealing tape (Sigma Aldrich Company, UK) and kept at -80°C until required for DIMS analysis.

Lipidomics was performed as described previously⁴¹ using chip-based nanospray with an Advion TriVersa Nanomate (Advion, Ithaca, USA) interfaced to the Thermo Exactive Orbitrap (Thermo Scientific, Hemel Hempstead, UK). Briefly, a mass acquisition window from 200 to 2000 m/z and acquisition in positive and negative modes were used with a voltage of 1.2 kV in positive mode and -1.5 kV in negative mode and an acquisition time of 72 s.

Acquired spectral raw data were processed as described previously⁴¹ using an in-house bioinformatics platform based on XCMS⁴². With the use of predefined rejection lists and mass defect filters, this performed sample-specific mass re-calibration using predefined sets of internal standards and the removal of commonly present contaminant ions (often associated with plasticizers). The raw data were converted to.mzXML (using

MScConvert⁴³ with peakpick level 1), parsed with R and 50 (scan from 20 to 70) spectra were averaged per sample using XCMS⁴², with a signal cutoff at 2000. The files were aligned using the XCMS^{42,44} grouping function using “mzClust” with a m/z -window of 22 ppm and a minimum coverage of 60%. Automated compound annotation was carried out using both an exact mass search in compound libraries as well as applying the referenced Kendrick mass defect approach. Signal normalisation was performed by summing the intensities of all detected metabolites to a fixed value to produce a correction factor for the efficiency of ionisation.

As described previously⁴⁵, exact masses were fitted to the lipid maps library and subsequently annotated to the peak. This converts initially roughly 4000 features (spectral regions associated with an analyte). These features were then considered within the parameters of our model, leading to 9 identified lipid species excluding isotopes.

Data modelling using Bayesian Statistical Methods. *Model justification.* The data recorded in the present study were naturally hierarchical: there were multiple measurements of each metabolite in each subject; yet for the present experiment, the aim was to identify those metabolites that were consistently affected by altitude across the entire study population. For this reason, we adopted a hierarchical approach to statistical modelling – specifically we fitted a hierarchical Bayesian model for each metabolite. This model comprised robust regression models (robust in that the residuals were modelled with a t -distribution⁴⁶) for each binned ¹H-NMR region or lipid variable at the participant level; the parameters from these regression analyses (specifically the slope and intercept, β_1 and β_0) were themselves modelled with normal distributions. Beyond the more general contrasts between using Bayesian over frequentist statistics (a recent discussion of which can be found here⁴⁷), several advantages are specific to this application. First, a full distribution of credible regression lines for each metabolite in each subject was generated. Second, by fitting the complete hierarchical model in a single step, and estimating all distributions simultaneously, the estimates of the regression lines for each individual subject are constrained by the overarching distribution of the lines for that metabolite, a phenomenon known as shrinkage^{48,49}. Hence slopes that are very unlikely for an individual subject (when the slopes for the remainder of the group are considered) are excluded unless compelling evidence exists in the data.

Despite the advantages, Bayesian statistics are computationally expensive. Therefore, simple frequentist hierarchical models were fitted initially to all variables in order to identify those variables likely to be of interest for further modelling (in other words, those metabolites whose mean slopes were not zero). Only those metabolites whose mean slopes (from simple hierarchical modelling) were $> \pm 1.96$ SDs from the mean were carried forward for full Bayesian modelling. These slopes were later compared to those derived using Bayesian methods and found to be reasonable estimates (Supplementary Fig. 5). Finally, Bayesian inference is somewhat different to frequentist approaches (e.g. there are no p -values). Hence, we adopted the criterion that metabolites should not include 0 in the high-density (95%) interval of the posterior distribution of z -transformed slopes. Together, this means that two levels of filtering were employed to ensure that only those slopes undergoing large degrees of change were considered.

Model details. The full Bayesian hierarchical model used here was described previously⁵⁰. A model was fitted for every metabolite of interest. Data were z -transformed before fitting to reduce correlation between slopes and intercepts (which presents difficulties for the MCMC algorithm used in JAGS). Each model comprised linear sub-models of the standard form fitted to the normalised metabolite measurements for each subject, using a t -distribution for the residuals. The distribution of parameters for the t -distribution (σ and ν , the normality parameter) were estimated once per metabolite, not for each subject. The slopes and intercepts from each of these models were themselves modelled using normal distributions with parameters μ_0 (the mean intercept), σ_0 (the standard deviation of the intercepts), μ_1 (the mean slope) and σ_1 (the standard deviation of the slopes). Hence for each metabolite, the modelling process generated distributions for σ , ν , μ_0 , σ_0 , μ_1 and σ_1 and – for each subject – distributions for β_1 and β_0 . Our primary interest was in the distributions of μ_1 . Non-informative priors were used for all parameters. Remembering that all data were z -transformed prior to analysis, all σ were given a broad prior uniform distribution (with parameters $L = 10^{-3}$ and $H = 10^3$ denoting the low and high limits), and ν a broad exponential distribution with a minimum of 1 and mean of 30 (at which point the distribution is approximately normal). For each normal distribution, μ was given a normal prior with parameters $M = 0$ and $S = 10$. Both the individual and group regression were assessed simultaneously and the individual regression lines constrained by the average regression lines.

Bayesian analysis was conducted using R and JAGS (Just Another Gibbs Sampler⁵¹ as described in Kruschke⁵⁰). All code is available in supplementary materials.

Identified metabolites were presented with corresponding identification codes from the human metabolome database (HMDB). In the case of certain lipids where HMDB identification was not available, chemical entities of biological interest (ChEBI) were included.

Calculation of Absolute Changes. For the aqueous phase metabolites, the binned ¹H-NMR spectral regions corresponding to an identified metabolite were assessed. The change in spectral intensity between LDN and EBC was calculated and from this the median % change derived. Given that this was a measure of spectral intensity, no absolute value such as concentration/ml plasma could be given for the change, instead arbitrary units were employed. The LDN and EBC values were also corrected to the LDN value, to give a normalised ratio of change. The same approaches were employed for assessment of the degree of change in lipid abundance, although this only included those definitively annotated lipids.

Statistical analysis. Analysis was performed in GraphPad Prism 7. The LDN and EBC values for SpO₂ and body weight data were abnormally distributed, as assessed using the D’Agostino-Pearson normality test. Therefore, a Wilcoxon matched-pairs signed rank test was employed for analysis.

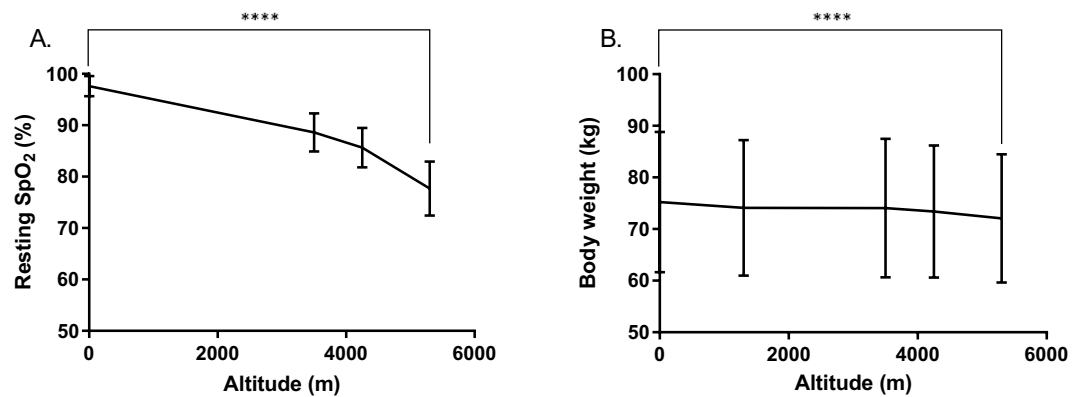


Figure 1. Changes in physiological variables with ascent to EBC. This includes recording of resting arterial O_2 saturation (SpO_2) (A) and body weight (kg) (B) at each time point upon ascent, with the midpoint representing the mean, \pm SD. Data was tested using a Wilcoxon matched-pairs signed rank test between LDN to EBC, **** $p < 0.0001$, $n = 146$ – 188 .

The Δ abundance of metabolites/lipids from LDN to EBC that were identified as undergoing large changes with ascent were plotted against the Δ SpO_2 or body weight from LDN to EBC. For the aqueous fraction metabolites, this specifically refers to the Δ of spectral region intensity undergoing the greatest change, and for lipids, the definitively identified lipid variables. Data that followed a Gaussian distribution were tested using a Pearson Correlation Coefficient. A non-parametric Spearman rank correlation (two tailed) was applied for non-normally distributed data. If a significant relationship was identified, linear regression analysis was subsequently performed.

Results

Subject Characteristics, Body Weights and Arterial O_2 Saturations. One hundred and ninety-eight participants (125 male, 73 female, 44 ± 14 (mean, \pm SD) years of age, BMI 25.1 ± 3.2 kg/m²) participated in the expedition to EBC³².

The degree of hypoxic exposure experienced at altitude was reflected through progressive decreases in resting SpO_2 with ascent. Overall, a 20.4% median decrease in SpO_2 ($n = 187$, $p < 0.0001$) from 98% at LDN to 78% at EBC was observed (Fig. 1A). Body weight also progressively fell by a median of 3.7% (3 kg) between LDN and EBC ($n = 157$, $p < 0.0001$), (Fig. 1B).

Plasma Metabolomic/Lipidomic Analysis. A total of 965 samples were obtained for metabolomic analysis on the aqueous fraction using NMR, and lipidomic analysis on the lipid fraction using DIMS. Between 182 and 198 samples were analysed from each altitude location, totaling up to 5 samples per volunteer (1 per altitude location). The reason for differences in sample number was due to participants failing to arrive at the laboratory³² or insufficient amounts of plasma being obtained for subsequent analysis. Bayesian robust hierarchical regression was used to identify metabolites that were robustly related to changes in altitude, from both the NMR and MS data. In particular, the focus was on those metabolites where the 95% high-density interval (a similar concept to 95% confidence intervals in traditional statistics) of estimates of the overall slope of metabolite abundance vs. altitude did not contain 0.

Plasma aqueous fraction analysis. An example of the Bayesian model output for the overall group response is displayed in Fig. 2A,B, with examples of the individual response being displayed in Supplementary Fig. 6. A summary of aqueous metabolite changes are outlined in Table 1, with differences in peak intensity from LDN to EBC, expressed as a ratio, presented in Fig. 3A. The changes include a progressive decrease in glucose (D-Glucose HMDB00122), an increase in lactate (L-Lactic acid, HMDB00190) and a decrease in the branched-chain essential amino acid isoleucine (L-Isoleucine HMDB00172) with ascent to EBC. From the spectral regions corresponding to these metabolites, specific spectral peaks undergoing the largest degree of change were identified as: 1.31ppm for lactate (27.4% increase), 3.35ppm for glucose (52.4% decrease) and 0.92 ppm for isoleucine (60.5% decrease).

Plasma lipid fraction analysis. Two examples of the output from Bayesian hierarchical modelling of lipidomic data of the full participant group are presented in Fig. 2C,D. All lipid species identified as undergoing large changes with ascent (defined in the same way as for NMR spectral regions, see above) are summarised in Table 2, with the LDN:EBC ratio presented in Fig. 3B. The largest % lipid increase was identified as triglyceride (TG) with carbon chain: double bond ratios of 52:3, with a median increase from LDN to EBC of 53.9%. This occurred alongside an increased TG 52:4 (CHEBI: 84660) and in the most abundant non-esterified fatty acids within adipose tissue. This includes the saturated palmitic acid (16:0) (HMDB00220) and unsaturated linoleic (18:2) (HMDB00673) and oleic (18:1) (HMDB00207) acids. An increase was also observed in sphingomyelin (SM) 34:2 (CHEBI:64587). The largest lipid % decrease was that of TG 48:1 (CHEBI: 85726), with a median decrease of 43.1%. This occurred alongside decreased TG 50:1 (50:1 (CHEBI: 84665) as well as phosphatidylcholine (PC) 46:2 (CHEBI: 72430).

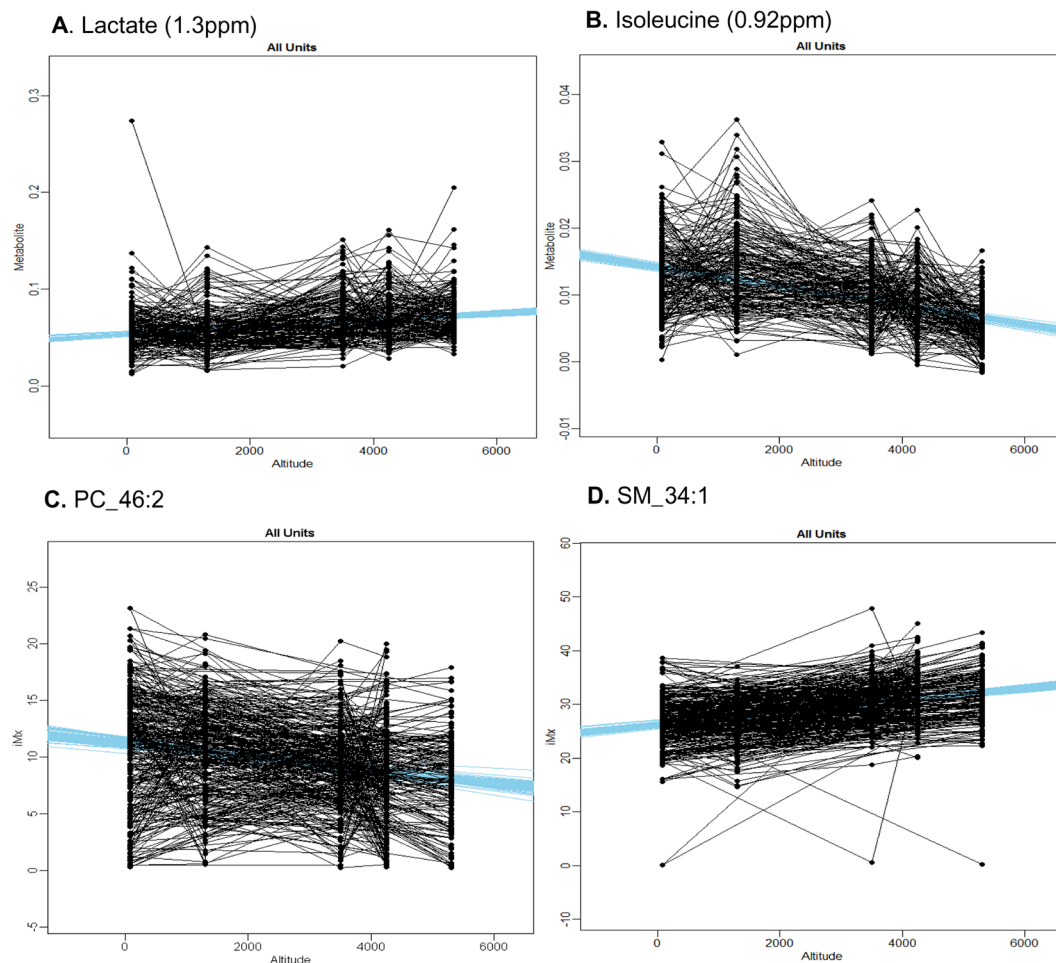


Figure 2. An example of the full subject group response of aqueous metabolites or lipids that demonstrate a significant trend with increasing altitude, identified using Bayesian hierarchical modelling. Example plots of lactate (A) and isoleucine (B), with corresponding $^1\text{H-NMR}$ regions, phosphocholine (PC) 46 carbons: 2 double bonds (46:2) (C) identified in negative ion mode and sphingomyelin (SM) 34:1 (D) identified in positive mode. Representative regression lines in blue have been drawn from the fitted distribution. This group distribution (all units) was informed from the most likely distribution at the level of the individual. Y axes metabolite units are arbitrary units, derived from the spectral intensity changing per km altitude.

Metabolite	Binned spectral region (ppm)	LDN intensity (AU)	EBC intensity (AU)	$\Delta\%$ LDN to EBC	Slope (AU/km)	Increasing or decreasing with altitude
Isoleucine	0.92	0.012	0.0049	-60.5	-0.00142	Decreasing
Glucose	3.35	0.016	0.0081	-52.4	-0.0014	Decreasing
Lactate	1.31	0.057	0.0719	27.4	0.00361	Increasing

Table 1. Spectral intensity, % change and credible regression slope change of the $^1\text{H-NMR}$ spectral regions identified as undergoing the largest degree of change with increasing altitude.

Correlation analysis. To assess whether a relationship existed between altitude dependent changes in metabolites/lipids from LDN to EBC and the specific physiological variables presented here, correlation plots were constructed.

Plots of changes in aqueous metabolites against body weight revealed a significant correlation between changes in glucose and body weight ($p = 0.007$), with decreased body weight being associated with decreased plasma glucose (Fig. 4A). Plots of the change in fatty acid vs. body weight from LDN to EBC revealed a significant correlation between the unsaturated oleic (18:1) ($p = 0.0127$) and linoleic (18:2) ($p = 0.0062$) FA's and body weight from LDN to EBC, with loss of body weight at altitude being associated with increasing levels of oleic and linoleic acids (Fig. 4B,C). No significant correlations were observed for changes in the other identified aqueous metabolites or lipids and body weight. Equally, no significance was observed between changes in any metabolite or lipid and SpO_2 .

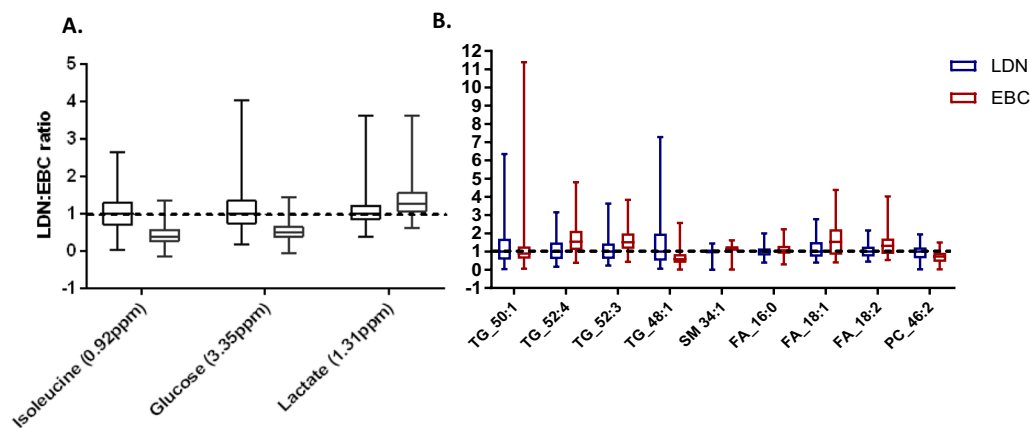


Figure 3. Alterations in aqueous metabolite and lipid abundance from London (LDN) to Everest base camp (EBC). Aqueous metabolite $^1\text{H-NMR}$ spectral regions (A) and lipids (assessed using DIMS) (B) undergoing the largest degree of change with ascent to EBC, identified using Hierarchical Bayesian statistics. Values are corrected to LDN, and so are expressed as a ratio of LDN: EBC, with a value of 1 indicative of no change. Presented as minimum to maximum box and whisker plots, with the middle line representing the median and the box the interquartile range (25th to 75th percentiles).

	Carbon chain length: double bond	Mode of ion detection	LDN abundance (AU)	EBC abundance (AU)	$\Delta\%$ LDN to EBC	Δ Slope (AU/km)
Lipids increasing with ascent						
Triglyceride	52:3	Positive	30.1	45.0	53.9	1.59
Triglyceride	52:4	Positive	10.72	16.50	53.7	0.529
Oleic acid	18:1	Negative	36.0	54.6	27.1	2.349
Linoleic acid	18:2	Negative	17.83	23.39	23.7	0.828
Sphingomyelin	34:1	Positive	26.8	30.8	15.7	0.001
Palmitic acid	16:0	Negative	110.4	116.7	12.4	2.176
Lipids decreasing with ascent						
Triglyceride	48:1	Positive	4.25	2.42	-43.1	-0.334
Phosphatidylcholine	46:2	Negative	11.8	8.7	-25.0	-0.597
Triglyceride	50:1	Positive	10.95	9.69	-8.43	-0.524

Table 2. Abundance, % change and credible regression slope change for lipid variables identified as undergoing the largest degrees of change with increasing altitude.

Discussion

With exposure to reduced PiO_2 during ascent to EBC, SpO_2 fell proportionally by $\sim 20\%$. We examined the metabolic response to this hypoxic exposure. We made efforts to distinguish this from responses to the inevitable potential confounders of an expedition of this nature, such as dietary changes. To this end, we used robust statistical methods to identify metabolites that changed with altitude and hierarchical methods that captured the full structure of the data. That these findings are consistent with known biology serves to validate the methods used.

Specific changes in aqueous metabolites include a decrease in the glycolytic substrate glucose alongside an increase in the glycolytic product lactate. This pattern of change has long been associated with increased glycolytic rate in the context of human cancer cell lines (e.g.⁵²). In the context of high altitude exposure, the changes observed support prior observations of decreasing blood glucose concentrations, increasing muscle glycolytic intermediates and increasing blood lactate levels in lowlanders ascending to high altitude^{6,8}. They are also in keeping with prior human, animal and cellular studies showing increased translocation of glucose transporters (GLUT-1 and GLUT-4) to the plasma membrane,^{53,54} upregulation of lactate dehydrogenase^{22,55} and a shunting of pyruvate away from entry into the TCA cycle and towards lactate formation⁹, all attributed to increased HIF-1 α activity. Together, this therefore suggests the changes observed are a result of increased reliance upon anaerobic glycolysis at rest following ascent to high altitude. However, it is also worth noting that a decrease in plasma glucose may result from increased insulin secretion, which has been shown previously to occur upon altitude exposure⁶.

Lipidomic analysis revealed alterations to the main constituent of body fat, TGs. Specifically, circulating levels of TGs 52:4 and 52:3 increased whereas TGs 50:1 and 48:1 decreased. Those TGs containing 48–50 carbons are typically associated with *de novo* lipogenesis a process by which excess carbohydrates are converted to fatty acids and subsequently to TGs for storage^{45,56}. This association has been demonstrated in human intervention studies⁴⁵.

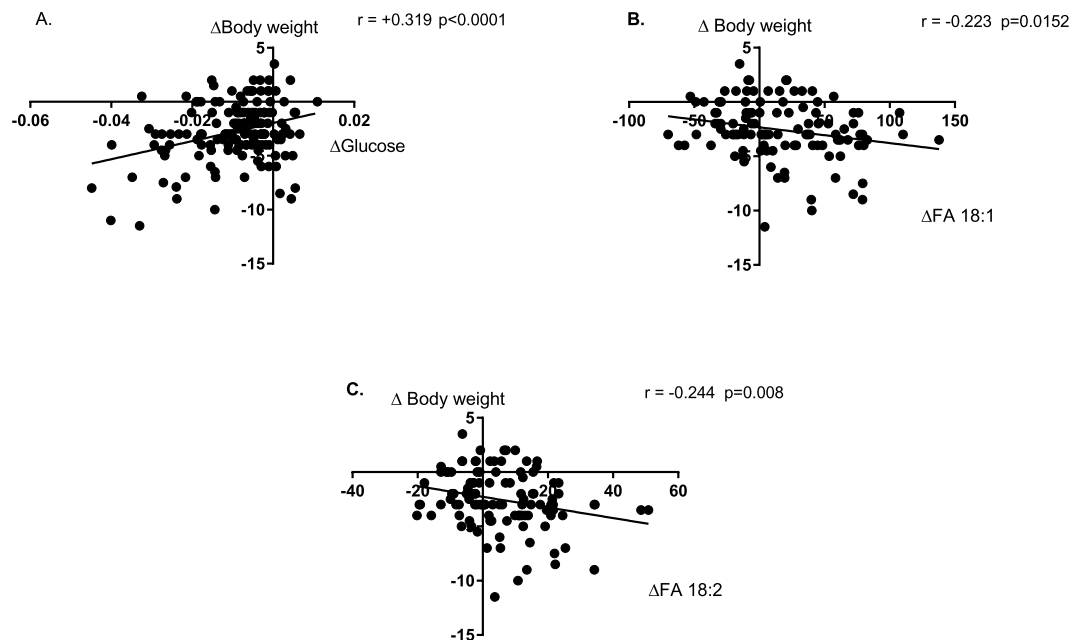


Figure 4. Correlation of Δ glucose or fatty acids (FA) vs. Δ body weight. Glucose (A), unsaturated FA 18:1 (B) and 18:2 (C), shown as carbon: double bond ratio. Δ calculated as EBC-LDN. Correlation analysis performed using Pearson rank correlation coefficient. Significant ($p < 0.01$) correlations analysed further using linear regression.

The fall in concentrations of TGs 48:1 and 50:1 with ascent to EBC may thus be linked with suppressed *de novo* lipogenesis, an effect known to be mediated by HIF-1 α ^{13,14}. The increase in TGs 52:4 and 52:3 are likely a compensatory change to retain a balance in circulating TGs. However, further analysis directly measuring *de novo* lipogenesis would be required to come to a firm conclusion regarding these changes.

The combination of decreased TGs alongside increased circulating levels of the most abundant fatty acids (including palmitic, linoleic and oleic acids), may be indicative of fat store mobilisation. This process can be induced via activation of the sympathetic nervous system (catecholamines activate cAMP-dependent phosphorylation of hormone sensitive lipase, which stimulates TG mobilisation⁵⁷). Sympathetic activation is known to occur in response to hypobaric hypoxia, with an increase in efferent activity directed towards the heart, kidneys, vasculature and skeletal muscle^{58,59}. Indeed, alterations in adrenaline/noradrenaline have been reported in previous investigations of the CXE expedition team, peaking at Namche Bazaar (3,500 m)⁶. Together this indicates that fat stores may become mobilised through hypoxic stimulated sympathetic activity, although again, further work would be required before a firm conclusion can be drawn.

Catecholamine stimulated breakdown of TGs to release fatty acids can be impaired through the action of insulin. Increased circulating levels of fatty acids (notably palmitic, oleic and linoleic acids) are associated with insulin resistance^{60–62}, including in models of obesity through a mechanism reliant upon c-Jun amino terminal kinases (JNKs)⁶³. Indeed, in a linked study by our group, participants remaining at EBC or above for prolonged periods exhibited a substantial increase in insulin and C-peptide⁶. It is therefore possible that the mobilisation of fat stores indicated in the present study, resulting in an increase in circulating fatty acids, is a causative factor for the spike in insulin concentrations observed in response to longer term exposure⁶.

The rise in circulating fatty acid levels may also contribute to previous reports of impaired β -oxidation capacity at high altitude⁵. Indeed, skeletal muscle mitochondrial respirometry carried out in a different cohort of lowlander participants undertaking similar ascent to that reported here, revealed impairment of skeletal muscle fatty acid oxidative phosphorylation at EBC along with an intramuscular accumulation of fatty acid intermediates⁸.

Lipidomic analysis also revealed changes in key membrane components, including a decrease in PC 46:2. PCs are key constituents in the construction of lipoproteins, in particular very low density lipoprotein (VLDL)⁶⁴, which is required for lipid transportation from the liver to cells. This observation may thus suggest that hypobaric hypoxia could affect this process. Disrupted lipoprotein transport, with inhibition of lipoprotein lipase activity in adipose tissue and pre-adipocytes, has been reported in response to chronic intermittent⁶⁵ and acute hypoxia⁶⁶, respectively.

An entirely novel change identified in the aqueous metabolites was a decrease in the essential branched-chain amino acid (BCAA) isoleucine with ascent. This is in contrast to prior studies investigating plasma responses of rats exposed to acute hypoxia (9.5% O₂, 5–18 hrs)⁶⁷ and in HeLa cells (1% O₂)⁶⁸, which reported an increase in isoleucine levels. This disparity may relate to differences in hypoxic exposure, with much more prolonged and progressive hypoxic exposure being adopted in our study, and the use of human participants.

In addition to their essential role in building muscle tissue, BCAAs are regulators of key cellular signaling pathways including that of the mammalian target of rapamycin (mTOR), a central regulator of cell metabolism,

growth and survival⁶⁹. The upregulation of mTOR signaling to induce protein synthesis is reliant upon an optimal ratio of BCAAs⁷⁰. In the present study, decreasing isoleucine levels were not matched by changes in the levels of leucine or valine to the same extent, as these amino acids did not meet the model criteria. Thus, whilst the consequences of the fall in circulating isoleucine in the context of hypoxic exposure remain to be determined, an impact upon muscle protein synthesis and potentially muscle catabolism, is likely. Indeed, mTOR protein levels have been reported to decrease in response to 7–9 days exposure to 4559 m in human vastus lateralis⁷¹.

In the present study body mass fell by an average of 3%, a finding in line with the commonly reported catabolic response to high altitude. First reported by Pugh in 1962⁷², a fall in body mass with altitude exposure has since been linked to loss of lean mass attributed to muscle catabolism^{73,74}. Attenuation of hypoxia-induced loss in body mass has been reported with BCAA supplementation⁷⁵, whereas supplementation solely with leucine was not effective⁷⁶. Together with the results of the present study, this may therefore suggest that inclusion of isoleucine in dietary supplementation may be crucial if muscle catabolism is to be mitigated against.

To investigate whether metabolite changes were associated with either the degree of change in SpO₂ or body weight with ascent, correlation analyses between metabolites/lipids and these factors were performed. This is in line with the notion that whilst changes in oxygen delivery are an essential part of hypoxic acclimatisation, alterations to metabolic processes modifying oxygen use at a cellular level are crucial^{5,8}. Indeed, mechanisms altering oxygen delivery do not account for inter-individual performance at altitude^{77,78} and the hypoxic phenotypes of acute mountain sickness does not correlate well with degree of SpO₂⁷⁹. Correlation analysis did reveal that loss of body weight was associated with decreasing plasma glucose and increasing oleic and linoleic acids. It is not possible to determine whether this association may be caused by dietary alterations or loss of appetite. However, it is important to note that the loss of body weight was associated with increasing altitude exposure, which is in line with previous work outlining that appetite suppression at altitude is a hypoxic driven response mediated by changes in leptin signaling^{80,81}. The present work thus highlights the importance of body mass changes with altitude in relation to metabolic shifts.

Study limitations. In comparison to previous studies examining metabolic acclimatisation of human subjects to high altitude hypoxia both in the field and laboratory, this study is unique in its scale and design. To enable success, it required the adoption of a pragmatic approach, the nature of which precluded the addition of a control group. Whilst the insult of hypobaric hypoxia was undoubtedly severe at the altitude reached, it must be noted that the effects reported may have been influenced by other environmental factors, such as a change in temperature and UV exposure.

Other factors that are known to impact metabolic function that may have affected the metabolomic/lipidomic profiles are potential alterations to exercise and diet. Daily activity data was not recorded, however all subjects underwent identical ascent profiles for which the exercise burden each day was low in both intensity and duration, as demonstrated by trekking distance/day detailed in the methods. Given that the cohort of subjects were healthy and active people, habitually partaking in exercise as part of normal life thus makes acute changes in exercise unlikely. In addition, the timing of the blood draw (rest day morning, minimum 16 hrs post exercise in a fasted, rested state), again makes effects of an exercise insult upon resulting metabolite/lipid analysis unlikely.

Dietary changes are another potential confounding factor, given that food was consumed *ad libitum* and was limited to that available in Kathmandu and the remote trekking locations. Had dietary effects been present, they would most likely become apparent between London and Kathmandu, and following this Kathmandu to Namche. Initial analysis performed on the data sets using PLS-DA models demonstrated that the most accurate, robust separation in lipid positive mode was apparent between London and EBC rather than the London, Kathmandu and Namche comparisons (Supplementary Fig. 7). In addition, the focus of the Bayesian model output is the regression line, along which is plotted each altitude location. Whilst fluctuations are apparent between altitude locations, the credible regression lines are shown to be robust to relatively minor shifts. Together, this suggests the major factor in influencing the direction of the resulting trend is altitude. However, we would recommend that future studies examining metabolomic/lipidomic profiles should include a standardised dietary intake, as well as a daily recording of exercise.

Finally, limitations of our statistical approach must be noted. The benefits of the robust Bayesian modelling approach have been outlined in the methods section. The downside of this is the vast computational power required. A compromise was therefore required to practically obtain results in a reasonable time scale, resulting in the model parameters outlined in the methods section. In addition to restricting computational power requirements, this approach also helped to focus analysis upon the 'big changers' within the profile. The restrictions placed upon the selection of those metabolites taken forward for Bayesian modelling may have limited metabolite/lipid identification. This was particularly apparent in the aqueous metabolite results whereby only 3 metabolites were taken forward. Such a compromise was considered worthwhile to ensure confidence in the data interpretation.

Conclusions

In summary, this study is the first to profile the systemic metabolic responses to increasing altitude in healthy humans, using untargeted metabolomics and lipidomics. Alterations identified in the aqueous fraction included the novel finding of decreasing isoleucine with ascent, with possible implications for muscle catabolism, alongside lactate and glucose changes that were in line with the well-documented increased reliance upon glycolytic energy metabolism. Fluctuations in the lipid profile with ascent suggest increased mobilisation of lipid stores and suppressed *de novo* lipogenesis. This occurred alongside changes to lipids that are essential membrane components, particularly those involved in the lipoprotein transport system. This study has therefore highlighted potential metabolic biomarkers for progressive hypoxic exposure in healthy humans.

Ethics approval and consent to participate. The study design, risk management plan and individual protocols for the Caudwell Xtreme Everest (CXE) Expedition were approved by the University College London

(UCL) Research Ethics Committee (in accordance with the declaration of Helsinki). Both verbal and written informed consent was obtained from all participants.

Data Availability

The datasets used and/or analysed during the current study are available from the corresponding authors on reasonable request.

References

- Tuder, R., Yun, J., Bhunia, A. & Fijalkowska, I. Hypoxia and chronic lung disease. *Journal of Molecular Medicine*. **85**, 1317–1324 (2007).
- Giordano, F. J. Oxygen, oxidative stress, hypoxia, and heart failure. *The Journal of clinical investigation*. **115**, 500–508 (2005).
- Center for International Earth Science Information Network - CIESIN - Columbia University, *National Aggregates of Geospatial Data Collection: Population, Landscape, And Climate Estimates, Version 2 (PLACE II)*, NASA Socioeconomic Data and Applications Center (SEDAC): Palisades, NY (2007).
- Peacock, A. J. Oxygen at high altitude. *BMJ: British Medical Journal*. **317**, 1063–1066 (1998).
- Horscroft, J. A. & Murray, A. J. Skeletal muscle energy metabolism in environmental hypoxia: climbing towards consensus. *Extreme Physiol Med*. **3** (2014).
- Siervo, M. *et al.* Effects of prolonged exposure to hypobaric hypoxia on oxidative stress, inflammation and gluco-insular regulation: the not-so-sweet price for good regulation. *PLoS One*. **9**, e94915 (2014).
- Ward, J. P. Oxygen sensors in context. *Biochimica et Biophysica Acta (BBA)-Bioenergetics*. **1777**, 1–14 (2008).
- Horscroft, J. A. *et al.* Metabolic basis to Sherpa altitude adaptation. *Proceedings of the National Academy of Sciences*. **114**, 6382–6387 (2017).
- Kim, J., Tchernyshyov, I., Semenza, G. L. & Dang, C. V. HIF-1-mediated expression of pyruvate dehydrogenase kinase: a metabolic switch required for cellular adaptation to hypoxia. *Cell metabolism*. **3**, 177–185 (2006).
- Semenza, G. L., Roth, P. H., Fang, H.-M. & Wang, G. L. Transcriptional regulation of genes encoding glycolytic enzymes by hypoxia-inducible factor 1. *Journal of biological chemistry*. **269**, 23757–23763 (1994).
- Young, P. M. *et al.* Operation Everest II: plasma lipid and hormonal responses during a simulated ascent of Mt. Everest. *Journal of Applied Physiology*. **66**, 1430–1435 (1989).
- Mahat, B., Chassé, É., Mauger, J.-F. & Imbeault, P. Effects of Acute Hypoxia on Human Adipose Tissue Lipoprotein Lipase Activity and Lipolysis. *The FASEB Journal*. **30**(758), 6–758.6 (2016).
- Menendez, J. A. & Lupu, R. Fatty acid synthase and the lipogenic phenotype in cancer pathogenesis. *Nature Reviews Cancer*. **7**, 763–777 (2007).
- Suzuki, T., Shinjo, S., Arai, T., Kanai, M. & Goda, N. Hypoxia and fatty liver. *World Journal of Gastroenterology: WJG*. **20**, 15087 (2014).
- Jiang, C. *et al.* Hypoxia-inducible factor 1 α regulates a SOCS3-STAT3-adiponectin signal transduction pathway in adipocytes. *Journal of Biological Chemistry*. **288**, 3844–3857 (2013).
- Jiang, C. *et al.* Disruption of hypoxia-inducible factor 1 in adipocytes improves insulin sensitivity and decreases adiposity in high-fat diet-fed mice. *Diabetes*. **60**, 2484–2495 (2011).
- Rankin, E. B. *et al.* Hypoxia-inducible factor 2 regulates hepatic lipid metabolism. *Molecular and cellular biology*. **29**, 4527–4538 (2009).
- Gibbons, G. F., Islam, K. & Pease, R. J. Mobilisation of triacylglycerol stores. *Biochimica et Biophysica Acta (BBA)-Molecular and Cell Biology of Lipids*. **1483**, 37–57 (2000).
- Cole, M. A. *et al.* On the pivotal role of PPAR α in adaptation of the heart to hypoxia and why fat in the diet increases hypoxic injury. *The FASEB Journal*, **201500094R** (2016).
- Simonson, T. S. *et al.* Genetic evidence for high-altitude adaptation in Tibet. *Science*. **329**, 72–75 (2010).
- Jacobs, R. A. *et al.* Mitochondrial function in human skeletal muscle following high-altitude exposure. *Exp Physiol*. **98** (2013).
- Green, H., Sutton, J., Cymerman, A., Young, P. & Houston, C. Operation Everest II: adaptations in human skeletal muscle. *Journal of Applied Physiology*. **66**, 2454–2461 (1989).
- Pollard, A. *et al.* Effect of altitude on spirometric parameters and the performance of peak flow meters. *Thorax*. **51**, 175–178 (1996).
- Pollard, A. J. *et al.* Hypoxia, hypocapnia and spirometry at altitude. *Clinical Science*. **92**, 593–598 (1997).
- Woods, D. R. *et al.* Insertion/deletion polymorphism of the angiotensin I-converting enzyme gene and arterial oxygen saturation at high altitude. *American journal of respiratory and critical care medicine*. **166**, 362–366 (2002).
- O'Brien, K. A. *et al.* Physiological and metabolic responses to prolonged hypoxia and extreme cold: Preliminary data from the White Mars Antarctica winter expedition. *Extreme Physiology & Medicine*. **4**, 1–2 (2015).
- Mamas, M., Dunn, W. B., Neyses, L. & Goodacre, R. The role of metabolites and metabolomics in clinically applicable biomarkers of disease. *Archives of toxicology*. **85**, 5–17 (2011).
- Murray, A. J. Metabolic adaptation of skeletal muscle to high altitude hypoxia: how new technologies could resolve the controversies. *Genome Med*. **1**, 117–117 (2009).
- Edwards, L. M. & Thiele, I. Applying systems biology methods to the study of human physiology in extreme environments. *Extreme Physiol Med*. **2** (2013).
- Tissot van Patot, M. C. *et al.* Enhanced leukocyte HIF-1 α and HIF-1 DNA binding in humans after rapid ascent to 4300 m. *Free Radical Biology and Medicine*. **46**, 1551–1557 (2009).
- Tissot van Patot, M. C. *et al.* Human placental metabolic adaptation to chronic hypoxia, high altitude: hypoxic preconditioning. *American Journal of Physiology-Regulatory, Integrative and Comparative Physiology*. **298**, R166–R172 (2010).
- Levett, D. Z. *et al.* Design and conduct of Caudwell Xtreme Everest: an observational cohort study of variation in human adaptation to progressive environmental hypoxia. *BMC medical research methodology*. **10**, 98 (2010).
- Beckonert, O. *et al.* Metabolic profiling, metabolomic and metabonomic procedures for NMR spectroscopy of urine, plasma, serum and tissue extracts. *Nature protocols*. **2**, 2692–2703 (2007).
- Curtis, K. J. *et al.* Acute Dietary Nitrate Supplementation and Exercise Performance in COPD: A Double-Blind, Placebo-Controlled, Randomised Controlled Pilot Study. *PLoS one*. **10**, e0144504 (2015).
- Savorani, F., Tomasi, G. & Engelsen, S. B. icoshift: A versatile tool for the rapid alignment of 1D NMR spectra. *Journal of Magnetic Resonance*. **202**, 190–202 (2010).
- Dieterle, F., Ross, A., Schlotterbeck, G. & Senn, H. Probabilistic quotient normalization as robust method to account for dilution of complex biological mixtures. Application in 1H NMR metabolomics. *Analytical chemistry*. **78**, 4281–4290 (2006).
- Keun, H. C. *et al.* Improved analysis of multivariate data by variable stability scaling: application to NMR-based metabolic profiling. *Analytica chimica acta*. **490**, 265–276 (2003).
- Karpievitch, Y. V., Nikolic, S. B., Wilson, R., Sharman, J. E. & Edwards, L. M. Metabolomics Data Normalization with EigenMS. *PLoS one*. **9**, e116221 (2014).
- Karpievitch, Y. V. *et al.* Normalization of peak intensities in bottom-up MS-based proteomics using singular value decomposition. *Bioinformatics*. **25**, 2573–2580 (2009).

40. Karpievitch, Y. V., Dabney, A. R. & Smith, R. D. Normalization and missing value imputation for label-free LC-MS analysis. *BMC bioinformatics*. **13**, S5 (2012).
41. Eiden, M. *et al.* Mechanistic insights revealed by lipid profiling in monogenic insulin resistance syndromes. *Genome Medicine*. **7**, 63 (2015).
42. Smith, C. A., Want, E. J., O'Maille, G., Abagyan, R. & Siuzdak, G. XCMS: processing mass spectrometry data for metabolite profiling using nonlinear peak alignment, matching, and identification. *Anal Chem*. **78**, 779–87 (2006).
43. Race, A. M., Styles, I. B. & Bunch, J. Inclusive sharing of mass spectrometry imaging data requires a converter for all. *J Proteomics*. **75**, 5111–2 (2012).
44. Tautenhahn, R., Böttcher, C. & Neumann, S. Highly sensitive feature detection for high resolution LC/MS. *BMC Bioinformatics*. **9**, 504 (2008).
45. Sanders, F. W. B. *et al.* Hepatic steatosis risk is partly driven by increased *de novo* lipogenesis following carbohydrate consumption. *Genome Biology*. **19**, 79 (2018).
46. Gelman, A. *et al.* Bayesian Data Analysis. Vol. 3e, New York: Chapman and Hall/CRC Press (2013).
47. Efron, B. A 250-year argument: Belief, behaviour, and the bootstrap. *Bulletin of the American Mathematical Society*. **50**, 129–146 (2013).
48. Kruschke, J. K. & Vanpaemel, W. Bayesian estimation in hierarchical models, In *The Oxford Handbook of Computational and Mathematical Psychology*, Oxford University Press, USA. p. 279 (2015).
49. Kruschke, J. K. What to believe: Bayesian methods for data analysis. *Trends in cognitive sciences*. **14**, 293–300 (2010).
50. Kruschke, J. K., *Doing Bayesian Data Analysis*. 2 ed.: Elsevier (2015).
51. Plummer, M. JAGS: A Program for Analysis of Bayesian Graphical Models Using Gibbs Sampling. In *Proceedings of the 3rd International Workshop on Distributed Statistical Computing (DSC 2003)*. Vienna, Austria (2003).
52. Galarraga, J. *et al.* Glucose metabolism in human gliomas: Correspondence of in situ and in vitro metabolic rates and altered energy metabolism. *Metabolic Brain Disease*. **1**, 279–291 (1986).
53. Xia, Y., Warshaw, J. B. & Haddad, G. G. Effect of chronic hypoxia on glucose transporters in heart and skeletal muscle of immature and adult rats. *American Journal of Physiology-Regulatory, Integrative and Comparative Physiology*. **273**, R1734–R1741 (1997).
54. Semenza, G. L. Regulation of mammalian O₂ homeostasis by hypoxia-inducible factor 1. *Annual review of cell and developmental biology*. **15**, 551–578 (1999).
55. Firth, J. D., Ebert, B. L. & Ratcliffe, P. J. Hypoxic regulation of lactate dehydrogenase A Interaction between hypoxia-inducible factor 1 and cAMP response elements. *Journal of Biological Chemistry*. **270**, 21021–21027 (1995).
56. Ameer, F., Scanduzzi, L., Hasnain, S., Kalbacher, H. & Zaidi, N. *De novo* lipogenesis in health and disease. *Metabolism*. **63**, 895–902 (2014).
57. Kraemer, F. B. & Shen, W.-J. Hormone-sensitive lipase control of intracellular tri-(di-) acylglycerol and cholesteryl ester hydrolysis. *Journal of lipid research*. **43**, 1585–1594 (2002).
58. Fisher, J. P., Flück, D., Hilty, M. P. & Lundby, C. Carotid chemoreceptor control of muscle sympathetic nerve activity in hypobaric hypoxia. *Experimental Physiology*. **103**, 77–89 (2018).
59. Guyenet, P. G. Neural structures that mediate sympathoexcitation during hypoxia. *Respiration Physiology*. **121**, 147–162 (2000).
60. Shen, W. & McIntosh, M. K. Nutrient Regulation: Conjugated Linoleic Acid's Inflammatory and Browning Properties in Adipose Tissue, In *Annual Review of Nutrition*, **36**, Stover, P. J. Editor. p. 183–210 (2016).
61. Shi, H. *et al.* TLR4 links innate immunity and fatty acid-induced insulin resistance. *The Journal of clinical investigation*. **116**, 3015–3025 (2006).
62. Benoit, S. C. *et al.* Palmitic acid mediates hypothalamic insulin resistance by altering PKC- θ subcellular localization in rodents. *The Journal of clinical investigation*. **119**, 2577–2589 (2009).
63. Hirosumi, J. *et al.* A central role for JNK in obesity and insulin resistance. *Nature*. **420**, 333–336 (2002).
64. Eisenberg, S. High density lipoprotein metabolism. *Journal of lipid research*. **25**, 1017–1058 (1984).
65. Drager, L. F. *et al.* Intermittent hypoxia inhibits clearance of triglyceride-rich lipoproteins and inactivates adipose lipoprotein lipase in a mouse model of sleep apnoea. *Eur Heart J*. **33** (2012).
66. Mahat, B., Chassé, É., Mauger, J.-F. & Imbeault, P. Effects of acute hypoxia on human adipose tissue lipoprotein lipase activity and lipolysis. *Journal of Translational Medicine*. **14**, 212 (2016).
67. Muratsubaki, H. & Yamaki, A. Profile of Plasma Amino Acid Levels in Rats Exposed to Acute Hypoxic Hypoxia. *Indian Journal of Clinical Biochemistry*. **26**, 416–419 (2011).
68. Troy, H. *et al.* Metabolic profiling of hypoxia-inducible factor-1 β -deficient and wild type Hepa-1 cells: effects of hypoxia measured by 1H magnetic resonance spectroscopy. *Metabolomics*. **1**, 293–303 (2005).
69. Laplante, M. & Sabatini, D. M. mTOR signaling at a glance. *Journal of Cell Science*. **122**, 3589–3594 (2009).
70. Duan, Y. *et al.* Free Amino Acid Profile and Expression of Genes Implicated in Protein Metabolism in Skeletal Muscle of Growing Pigs Fed Low-Protein Diets Supplemented with Branched-Chain Amino Acids. *Journal of Agricultural and Food Chemistry*. **64**, 9390–9400 (2016).
71. Viganò, A. *et al.* Proteins modulation in human skeletal muscle in the early phase of adaptation to hypobaric hypoxia. *Proteomics*. **8**, 4668–4679 (2008).
72. Pugh, L. G. C. E. Physiological and Medical Aspects of the Himalayan Scientific and Mountaineering Expedition. *British Medical Journal*. **2**, 621–627 (1962).
73. Wandrag, L. *et al.* Does hypoxia play a role in the development of sarcopenia in humans? Mechanistic insights from the Caudwell Xtreme Everest Expedition. *Redox Biology*. **13**, 60–68 (2017).
74. Murray, A. J. & Montgomery, H. E. How wasting is saving: Weight loss at altitude might result from an evolutionary adaptation. *BioEssays*. **36**, 721–729 (2014).
75. Schena, F., Guerrini, F., Tregnaghi, P. & Kayser, B. Branched-chain amino acid supplementation during trekking at high altitude. *European Journal of Applied Physiology and Occupational Physiology*. **65**, 394–398 (1992).
76. Wing-Gaia, S. L., Gershenoff, D. C., Drummond, M. J. & Askew, E. W. Effect of leucine supplementation on fat free mass with prolonged hypoxic exposure during a 13-day trek to Everest Base Camp: a double-blind randomized study. *Applied Physiology, Nutrition, and Metabolism*. **39**, 318–323 (2013).
77. Martin, D. S., Levett, D. Z. H., Grocott, M. P. W. & Montgomery, H. E. Variation in human performance in the hypoxic mountain environment. *Experimental Physiology*. **95**, 463–470 (2010).
78. Cerretelli, P. Limiting factors to oxygen transport on Mount Everest. *Journal of Applied Physiology*. **40**, 658–667 (1976).
79. O'connor, T., Dubowitz, G. & Bickler, P. E. Pulse Oximetry in the Diagnosis of Acute Mountain Sickness. *High Altitude Medicine & Biology*. **5**, 341–348 (2004).
80. Shukla, V. *et al.* Ghrelin and leptin levels of sojourners and acclimatized lowlanders at high altitude. *Nutritional Neuroscience*. **8**, 161–165 (2005).
81. Tschöp, M., Strasburger, C. J., Hartmann, G., Biollaz, J. & Bärtsch, P. Raised leptin concentrations at high altitude associated with loss of appetite. *The Lancet*. **352**, 1119–1120 (1998).

Acknowledgements

CXE is a research project coordinated by the Centre for Altitude, Space and Extreme Environment Medicine, University College London, UK. The CXE Research Groups members all contributed to the collection of the data described in this study. Membership, roles and responsibilities of the CXE Research Group can be found at <http://www.caudwell-xtreme-everest.co.uk/team>. The CXE expedition was funded from a variety of sources, none of which are public. The entrepreneur John Caudwell, whose name the expedition carries, donated £500,000 specifically to support the research. BOC Medical, now part of the Linde Group, generously supported the research early on and continues to do so. Ely-Lilly Critical Care, The London Clinic (a private hospital), Smiths Medical, Deltex Medical and Rolex also donated money to support the research and logistics. All monies were given as unrestricted grants. Specific research grants were awarded by the Association of Anaesthetists of Great Britain and Ireland, and the UK Intensive Care Foundation. The CXE trekkers themselves also kindly donated to support the research. H.E.M. and M.G.M. are supported by the National Institute for Health Research (NIHR) University College London Hospitals Biomedical Research Centre, London, UK. M.P.W.G., D.Z.H.L. and K.M. are supported by the National Institute of Health Research (NIHR) University Hospital Southampton Biomedical Research Centre, Southampton, UK. A.J.M. received an Academic Fellowship from the Research Councils UK (EP/E500552/1). Work in the JLG lab is funded by the Medical Research Council (Lipid Profiling and Signalling; MC_UP_A090_1006). KAO was funded by King's College London on a Graduate Teaching Assistant PhD studentship.

Author Contributions

A.J.M., D.S.M., D.Z.L., M.K., M.G.M., H.E.M. and M.P.W.G. were all involved in initiating the study design and conduct of C.X.E. Experimental design for the blood processing and analysis presented here was conducted by K.A.O., L.M.E., J.L.G., A.J.M. and M.P.W.G. Blood separation and preparation was performed by K.A.O., ¹H.-N.M.R. and D.I.M.S. runs were conducted by A.A. and L.R., respectively. Data pre-processing was performed by K.A.O. and A.K. Statistical analysis was performed by L.M.E. and K.A.O. The manuscript was written by K.A.O., S.D.R.H., J.L.G. and L.M.E. and was approved and edited by all authors. Senior authors L.M.E., J.L.G., M.P.W.G. each provided equal contribution to the manuscript.

Additional Information

Supplementary information accompanies this paper at <https://doi.org/10.1038/s41598-019-38832-z>.

Competing Interests: The authors declare no competing interests.

Publisher's note: Springer Nature remains neutral with regard to jurisdictional claims in published maps and institutional affiliations.



Open Access This article is licensed under a Creative Commons Attribution 4.0 International License, which permits use, sharing, adaptation, distribution and reproduction in any medium or format, as long as you give appropriate credit to the original author(s) and the source, provide a link to the Creative Commons license, and indicate if changes were made. The images or other third party material in this article are included in the article's Creative Commons license, unless indicated otherwise in a credit line to the material. If material is not included in the article's Creative Commons license and your intended use is not permitted by statutory regulation or exceeds the permitted use, you will need to obtain permission directly from the copyright holder. To view a copy of this license, visit <http://creativecommons.org/licenses/by/4.0/>.

© The Author(s) 2019